PREDICTIONS AND MEASUREMENTS OF THE VISCOELASTIC RESPONSE OF UNIDIRECTIONAL FIBRE COMPOSITES

Mehtab V. Pathan[1], Sophoclis Patsias[2] and Vito L. Tagarielli[1]

[1] Department of Aeronautics, Imperial College London, South Kensington Campus, London SW7 2AZ, UK
[2] Rolls-Royce plc, PO Box 31, DE24 8BJ, UK

Email: m.pathan13@imperial.ac.uk

Keywords: Fibre-composites, Damping, Finite Element Method, RVE

ABSTRACT

Composite materials are increasingly being used in the aerospace industry due to their excellent specific stiffness and strength in conjunction with their higher vibration damping capacity. However, obtaining accurate numerical prediction of their mechanical properties is still an issue, instead designers rely on experimental characterization methods which are costly and time consuming. In this paper, we perform finite element analysis of the mechanical response of random RVEs representing the microstructure of a unidirectional (UD) fibre composite, predicting its anisotropic stiffness and damping properties and studying their sensitivity to temperature and frequency, using as inputs only the measured response of the constituents. The numerical predictions were found to be in reasonable agreement with experiments and the present approach was found to provide more accurate predictions than existing theoretical models. Based on the numerical predictions, a new simple interpolative analytical model has been proposed to predict the viscoelastic response of FRPs.

1 INTRODUCTION

Aerospace components are exposed to significant vibratory loading during their operation, hence materials with higher damping characteristics are desirable. Unlike metallic structures, composite laminates exhibit higher inherent damping due to the viscoelastic nature of matrix thus negating the need of additional damping treatments such as viscoelastic inserts, resulting in weight saving. The macroscopic mechanical response of FRPs is a function of various parameters such as the fibre volume fraction, constituent properties and their microstructure; as well as temperature and imposed loading frequency. Experimental investigation over such a large space of design variables is time consuming and requires specialist equipment. Therefore, a fast numerical tool is required to provide accurate predictions using as inputs only the measured properties of the constituent materials, to allow an assessment of the composite's response prior to manufacturing.

Damping properties of fibre composites can be tailored by controlling different parameters at both microscopic level (constituent materials, fibre volume fraction, fibre aspect ratio) and at laminate level (stacking sequence). In the existing literature the investigation on damping of fiber composites has been largely restricted to analysis of laminates [1,2]. Studies addressed at the microscopic levels are largely limited to the analysis of periodic unit cells [3,4]. However, Tsai and Chi [5] and Pathan et al [6] assessed the effect of different periodic arrangement of fibers on damping and found the loss factors to be strongly dependent on the spatial distribution of the fibers. Hence, high fidelity numerical models considering random distribution of fibres are required to get accurate prediction of the anisotropic viscoelastic response of FRPs. Moreover, much of the published research investigated *either* the elastic properties *or* the damping properties; numerical comparison of predictions to experiments is very often conducted on the response of laminates rather than that of single plies, making validation of the predictions difficult. Existing experimental studies come to contrasting conclusions and measurements of damping of similar materials may differ by up to an order of magnitude. Further, limited studies have addressed the dependence on frequency and temperature.

In this study, we conduct measurements of the viscoelastic properties of individual carbon fibers, of a selected epoxy resin and of the resulting unidirectional (UD) composite of these two materials, produced by vacuum infusion. Numerical prediction of the homogenized viscoelastic response of FRPs is obtained by performing Monte-Carlo simulations on representative volume elements (RVE), using the measured properties of the constituents. Predictions are conducted as a function of the imposed frequency and temperature and for several loading cases, in order to fully populate the transversely isotropic viscoelastic stiffness tensor of the UD composite. Numerical predictions are compared to the DMTA measurements as well as to other state-of-the-art theoretical models. The accuracy of such models is discussed and a new interpolative model is proposed to conduct inexpensive predictions of the anisotropic viscoelastic response of UD laminae. The outline of the paper is as follows: in Section 2 we discuss the manufacturing of the composite and the testing methods. Section 3 presents the details of the numerical models, while results are discussed in Section 4.

2 EXPERIMENTAL METHODS

2.1 Material manufacturing

A neat Prime20 LV resin/slow hardener panel was manufactured using the vertical sandwich panel method[7], to minimize air bubbles in the specimen. The resin mixture was degassed and cured in oven at 50 °C for 16 hr, according to the manufacturer's instructions. Beams of size $50\times6\times2$ mm were manufactured using a water jet cutter and conventional milling. The glass transition temperature (corresponding to a peak of loss factor) was found to be 81 °C via a DMTA temperature sweep test (soak time of 5 mins, temperature ramp rate of 1 C/min); this value is in good agreement with the manufacturer's value of 82.6 °C.

Elastic and damping properties of the T700 carbon fibres employed in this study were measured using single fibre tests, following ASTM C1557-14 standard. Single fibres were randomly pulled from a bundle and mounted on a paper tab using a thin layer of a two-part epoxy adhesive. Fibre diameter of each specimen was then measured using an optical microscope. The specimens were tested using flat-faced tensile grips in a DMTA; the gauge length was limited to 30 mm due to the limitations of the apparatus.

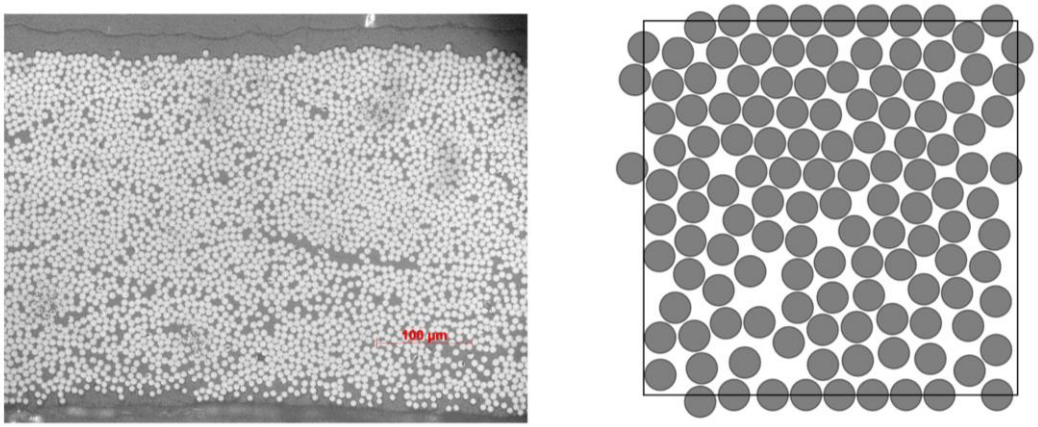

Figure 1: (a) Microscopic image showing composite cross section of norimal $\phi_f = 0.63\%$, and (b) example of an analysed virtual microstructure with same fibre volume fraction and $\delta = 24$.

A UD fibre composite plate measuring 300×300 mm was manufactured using three layers of T700 fibre fabric (Sigmatex UK, 150 gsm, 12K) and Prime20LV/Slow using the resin infusion under flexible

tooling method. The panel was cured at atmospheric pressure for 16 hrs at 50 °C, i.e. in identical conditions as for the neat resin. The fibre volume fraction, void fraction and nominal thickness of the specimen were measured using image analysis of micrographs obtained using an optical microscope. The measured fibre volume fraction was 63%, the average fibre diameter was $6.77\,\mu m$, with a standard deviation of $0.335\,\mu m$. Beams of size $50\times 6\,mm$ were extracted from the plate such that the longitudinal axis of the beam formed angles of 0°, 90° and 45° with the fibre direction.

The micrograph in Fig. 1a shows a resin region at the top of the composite plate; this represents a section of the resin-rich pattern left on the plate by the resin infusion mat used in the manufacturing. This influenced the thickness of the specimen, which was irregular and varied periodically in the plane of the plate, measured at an average of 0.32 mm using several micrographs. The resin rich layer on average consisted of around 8% of the total specimen thickness.

2.2 Mechanical testing

Measurements of the stiffness and damping properties of the constituents and the UD composite were performed by the forced vibration (non-resonant) technique, making use of a DMTA analyzer(RSA-G2 by TA instruments) with load capacity of 35 N. Isothermal frequency sweeps in the range 0.1-10 Hz were conducted at three different temperatures (25, 40 and 50°C). Tests on the single carbon fibres were performed in axial mode while measurements on the neat resin and on the composite beams were performed in three-point bending configuration, due to the limited load capacity of the DMTA.

2.2.1 Response of the neat resin

Tests on epoxy beams were performed using a pre-load of 1 N and a strain amplitude of 0.04%. Five samples were tested at the three selected temperatures and the response was found to be repeatable within a 10% margin; Fig. 2 shows averages of the storage modulus and the loss factor of the matrix measured in the DMTA experiments. Note that the loss factor is defined as the ratio between the imaginary and real parts of the complex modulus. The storage modulus and loss factor are sensitive to frequency and temperature; the modulus increases monotonically with the applied frequency (i.e., strain rate); the loss factor decreases with frequency, as expected for viscoelastic materials in glassy region. An increase in temperature results, as expected, in a decrease of storage modulus and an increase in the loss factor in a non-linear manner.

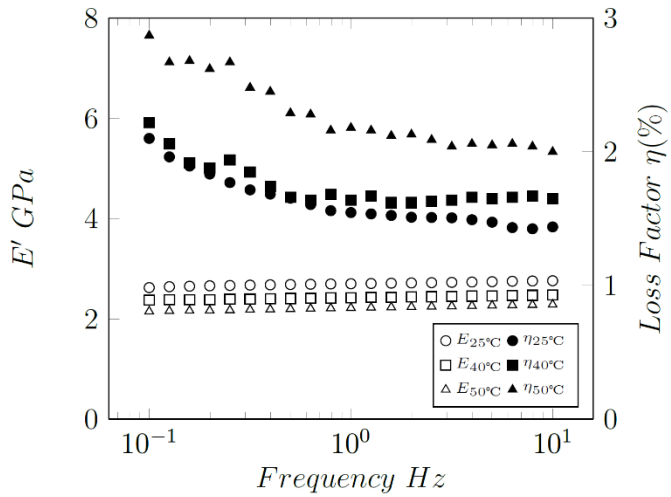

Figure 2: Stiffness and damping properties of neat resin as a function of loading frequency at 25, 40 and 50 °C.

2.2.2 Response of the single carbon fibres

The longitudinal damping of UD fibre composites is substantially influenced by the damping of the fibres, which is often neglected in the literature on the ground that loss factors for fibres are typically one order of magnitude lower than those of the matrix. Frequency sweep on single carbon fibre specimen was performed using a pre-load equal to 0.08 N, with an imposed strain amplitude of 0.1%. The mean measured storage modulus of 225 GPa is in good agreement with the value reported by the manufacturer (230 GPa); the scatter in modulus was upto7%. The loss factor of the fibres had a mean of 0.0033 but showed a greater variation around this value, of the order 100%. Following the findings of Saunder et al. [8] and Feih and Mouritz [9], the temperature dependence of storage modulus and loss factors of carbon fibre was neglected.

2.2.3 Anisotropic response of the UD composite

The UD composite was tested along three different directions, such that fibres were oriented longitudinally, transversely and at 45° with respect to the axis of the beam. Following a strain amplitude sweep, frequency sweeps were conducted in the range 0.1-10 Hz, with a strain amplitude of 0.02%. Again, tests were performed at the temperatures of 25, 40 and 50 °C.

Experiments were repeated 5 times and the averages of the measurements are presented in Figs. 3-8; Figures 3-5 compare the measurements at 25 °C to existing analytical models and numerical predictions described below; Figures 6-8 show measurements and numerical predictions of the response at different temperatures. As expected it was found that, for all orientations, storage moduli increase and loss factors decrease with increasing frequency, as visible in Figs. 3-5. Conversely, an increase in the test temperature resulted in a decrease of storage moduli and an increase in loss factors (see Figs. 6-8).

3. NUMERICAL ANALYSIS

3.1 Generation of the random RVEs

Virtual microstructures of the UD composite were generated using an algorithm based on optimization techniques, previously proposed by the authors [10]. Mechanical analysis [6] revealed that in order to obtain predictions of the viscoelastic properties that are insensitive to SVE size, and associated to a scatter of less than 5%, it is necessary to analyze RVEs of size $\delta = L/R \geq 24$; which is used in this study. These RVEs have thickness, $t = 4R$ along the fibre direction, as it was previously shown in [11] that predictions are insensitive to *t* for $t > 4R$. The mean radius of the carbon fibres was measured as $6.77\ \mu\text{m}$, by performing image analysis on optical micrographs. Example of an analysed RVE of $\phi_f = 0.63$ and $\delta = 24$ is given in Fig. 1(b). A total of 10 repeated simulations were performed, in each case, on different realizations of the microstructure.

3.2 Details of the FE simulations

Analyses of the response in the frequency domain were conducted with the commercial FE software Abaqus/standard , performing periodic steady-state analysis. The RVEs were subjected to three different harmonic loading cases, i.e. uniaxial stress along the fibres and in the transverse direction, as well as axial shear. The macroscopic strains imposed on the RVEs were pure sine waves of amplitude arbitrarily set to 0.01 and varying frequencies. The analysis allowed calculation of the corresponding macroscopic stress histories; such histories were interpreted as phasors and split into two components, in-phase (storage component) and out-of-phase (loss component) with respect to the imposed strain. The ratio of the in-phase stress amplitude to the corresponding strain amplitude provided the values of the storage moduli; similarly, the ratio of the out-of-phase stress amplitude to the strain amplitude gave the imaginary (or loss) modulus.

The microstructures were meshed using a combination of hexahedral and tetrahedral finite elements with linear shape functions (C3D8 and C3D6). A mesh sensitivity study was performed to determine the optimal element size in each loading case, to guarantee mesh-insensitive predictions. Periodic boundary conditions are known to give most accurate prediction for a given RVE size and hence were used in this study.

For a linear viscoelastic solid, the shear and volumetric response are independent and characterized by the complex shear and bulk modulus, G^* and K^*, or equivalently by the shear storage modulus $G^{'}$, the corresponding shear loss factor η_G, the bulk storage modulus $K^{'}$ and the volumetric loss factor n_K, where the following identities hold

$$G^* = G^{'}\left(1+i\eta_G\right);\ K^* = K^{'}\left(1+i\eta_K\right). \tag{1}$$

The matrix was modelled as isotropic viscoelastic solid and the damping response was assumed to be same in both dilation and shear i.e. $\left(\eta_K{}^m = \eta_G{}^m\right)$. The frequency and temperature dependence of the matrix were explicitly modelled by providing frequency- and temperature-dependent modulus and loss factors, according to the measurements in Fig. 2. Three sets of simulations were performed imposing a uniform temperature field of 25, 45 and 50 °C, as in the experiments. The Poisson's ratio of the polymeric matrix was taken as $\nu_m = 0.38$ and was assumed to be independent of temperature and frequency for the given testing range. The fibres were modelled as transverse isotropic elastic solid with isotropic damping (i.e. $\eta_{11} = \eta_{22} = \eta_{12} = \eta_{23}$ in the usual notation). The measured axial fibre modulus is used to calibrate the constitutive model; due to difficulties in measuring the transverse Young's modulus of carbon fibre, $E^{'}_{22f}$ was taken as 25 GPa i.e. ($\approx 10\%\ E^{'}_{11f}$) with $G^{'}_{23f} = 9.62\,\text{GPa}$, $G^{'}_{12f} = 40\,\text{GPa}$ and $\nu_{12f} = 0.2$. An Abaqus user material interface (UMAT) was developed to implement the linear viscoelastic constitute response in the frequency domain.

4. RESULTS AND DISCUSSION

In this section we compare the DMTA measurements to the numerical predictions and to a number of established theoretical models. We begin by considering measurements and predictions of the response to frequency sweeps at a temperature of 25°C; then, we examine separately the effects of an increasing temperature on the material response. Here we choose to assess the following models: (i) a direct rule of mixture (ROM) (ii) an inverse rule of mixtures (IROM);(iii) upper and lower bounds developed by Hashin [12] and Hill[13] (denoted as (Hashin+, Hashin- in the following, respectively); (iv) a model developed by Mori and Tanaka[14] (denoted as Mori-Tanaka), and (v) a model developed by Lielens (Lielens, [15]). We stress here that in the following, we provide ensemble averages of the FE predictions; the scatter in these predictions did not exceed 5%, as discussed in Section 3.1.

4.1 Anisotropic viscoelastic response of UD composite ply at 25°C

Measurements and numerical predictions of the material response at 25°C and frequency in the range 0.1-10 Hz are presented in Figs. 3-5. The figures include theoretical predictions from the models detailed in Section 4. Figure 3 refers to loading in the fibre direction (or direction 1); the axial storage modulus (fig. 3a) is scarcely dependent upon frequency and temperature in the ranges explored, as expected, and in good agreement with the FE simulations and all theoretical predictions shown in the figure. The corresponding measured axial loss factor (Fig. 3b) shows significant scatter and appears scarcely sensitive to frequency; the simulations agree with all the theoretical models shown, but appear to underestimate the loss factor with an error of around 15-20%.

We anticipate that for all load cases, the measured loss factors of the UD composite will be slightly higher than the corresponding numerical predictions, since in the real tests, other dissipative mechanisms such as aerodynamic damping due to surrounding air and frictional losses at clamps exist, in addition to the internal viscosity of the material. Friction between the loading fixture of the DMTA and the material specimens can be considerable, in consideration of the very small volume of the composite specimens, but is difficult to quantify. The discrepancy of 15-20% between predicted and measured damping is small compared to previously published studies. We conclude that our simulations predict correctly the axial loss factor.

The results for transverse loading are presented in Fig. 4. The measured storage modulus in direction 2 is in excellent agreement with the numerical predictions (Fig. 4a). In contrast, none of the theoretical models provides effective predictions of the transverse modulus; experimental results lie roughly mid-way between the predictions of the Lielens and Mori-Tanaka models. The measurements of transverse loss factor show significant scatter and are scarcely sensitive to the imposed frequency. The corresponding numerical predictions are in good agreement with the measurements (again, the FE simulations slightly underestimate the measurements) while again the theoretical models fail to predict accurately this material property; the Mori-Tanaka model provides the most accurate predictions.

For the case of the axial shear modulus, shown in Fig. 5a, we find that the experiments are again in broad agreement with the FE predictions, while the theoretical models fail to estimate the transverse storage modulus; both measurements and FE predictions show clear frequency dependency, with the modulus increasing with frequency. Figure 5b presents predictions and measurements of the axial shear loss factor; the experiments are in good agreement with the FE predictions. The IROM bound, the Hashin's lower bound and the Mori-Tanaka model provide reasonably good results, while Lielens model underestimates the loss factors. The measurements and the FE predictions show a decreasing shear loss factor with increasing frequency.

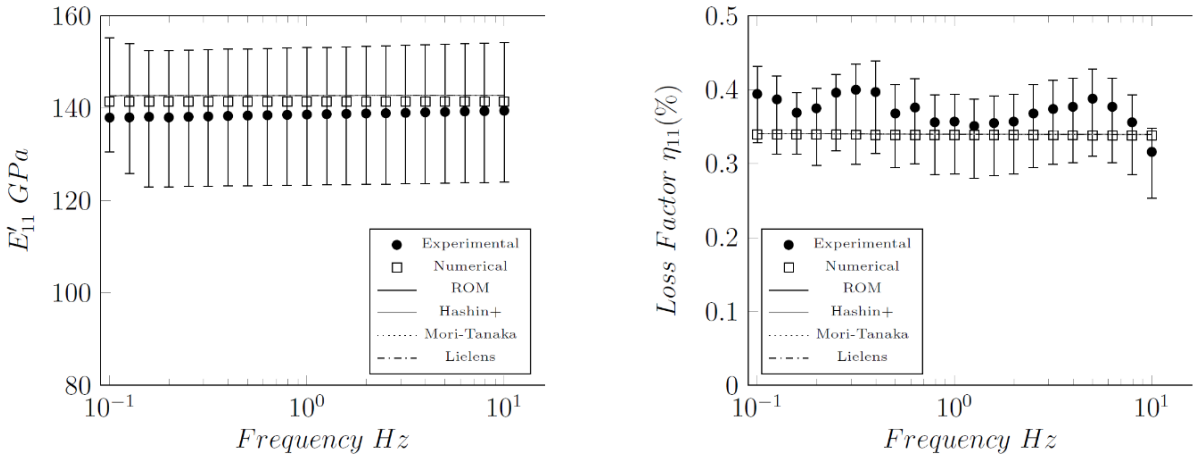

Figure 3: Comparison of the axial viscoelastic properties of UD CFRP as a function of loading frequency using numerical, experimental and analytical approaches; (a) Axial Young's modulus E'_{11} ; (b) Corresponding loss factor η_{11}.

4.2 Effect of temperature on the anisotropic viscoelastic response.

We proceed to examine the sensitivity of the measurements and FE predictions to temperature, by comparing the average measurements to the ensemble averages of the FE predictions in Figs. 6-8; the predictions of theoretical models are not included in the figures for the sake of clarity.

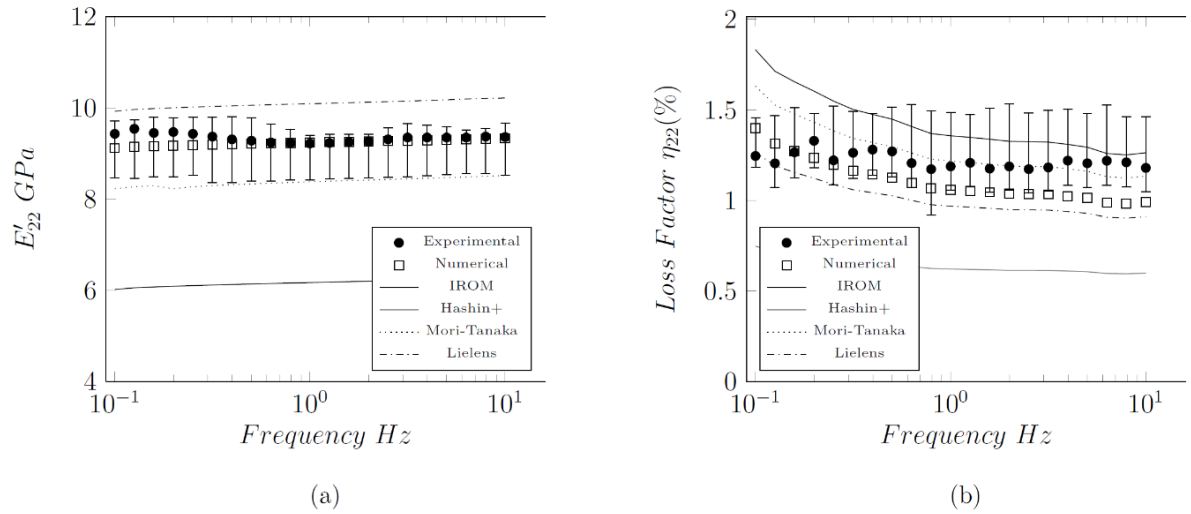

Figure 4: Comparison of the transverse viscoelastic properties of UD CFRP as a function of loading frequency using numerical, experimental and analytical approaches; (a) transverse Young's modulus E'_{22} ; (b) Corresponding loss factor η_{22} .

For the case of axial loading we find that FE predictions and measurements of the axial storage modulus (Fig. 6a) are in broad agreement; however, the FE predictions are insensitive to temperature and frequency, while the measurements show a small sensitivity to temperature (with the storage modulus decreasing with increasing temperature). Similar results are observed for the corresponding loss factor, shown in Fig. 6b. The sensitivity of axial viscoelastic properties to temperature is unexpected, as the axial response is dominated by fibre properties, which are known to be insensitive to temperature in the range explored. The measurements shown in Fig. 6a were conducted by clamping the specimens when both specimens and fixtures were at the correct test temperature; this practice reduced the sensitivity of the measured modulus to the test temperature. The measured sensitivity to test temperature might have been due to the presence of a resin-rich, irregular layer on the surface, as shown in in Fig. 1a.

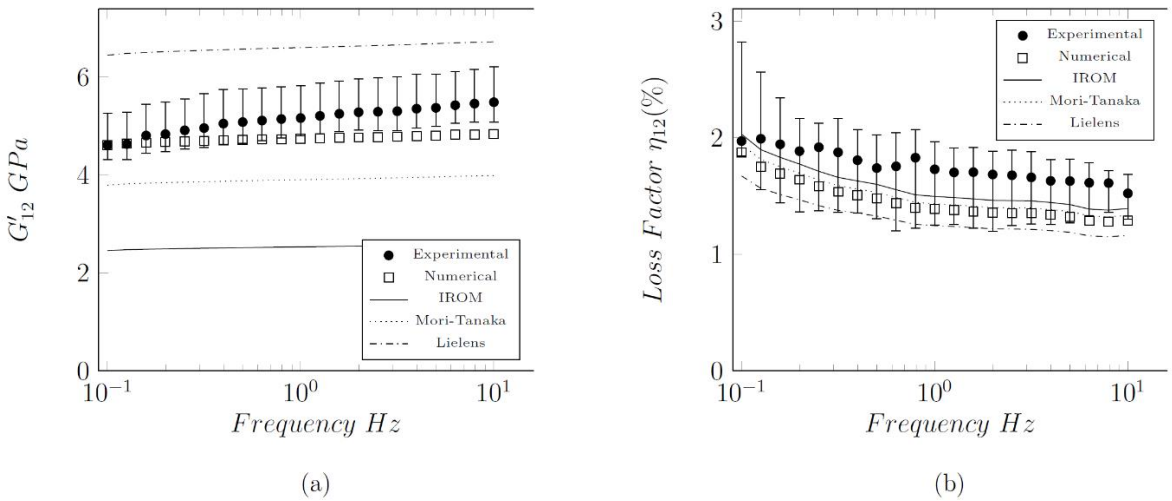

Figure 5: Comparison of the axial shear viscoelastic properties of UD CFRP as a function of loading frequency using numerical, experimental and analytical approaches; (a) axial shear modulus G'_{12} ; (b) Corresponding loss factor η_{12} .

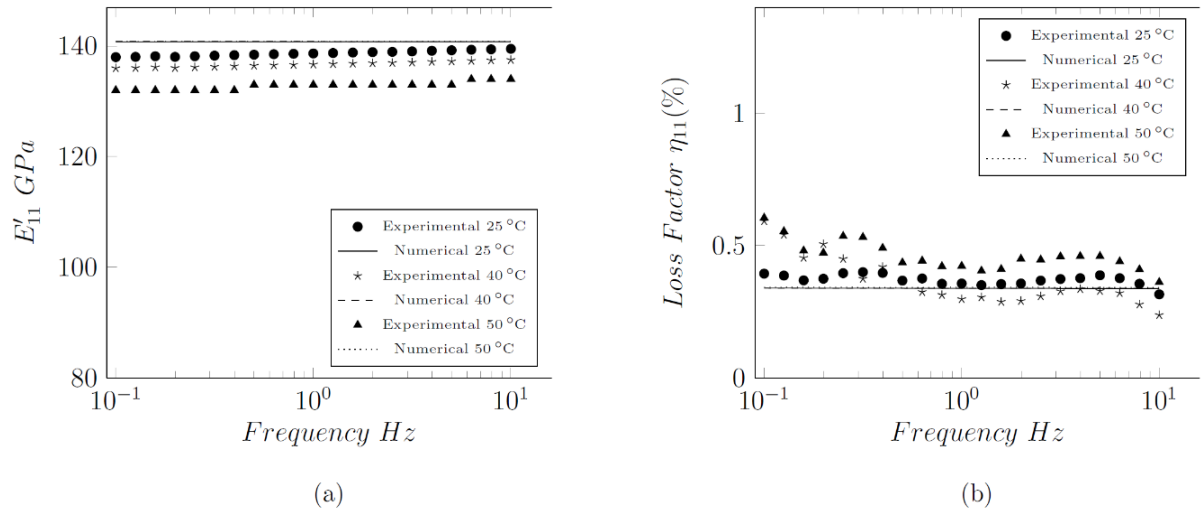

Figure 6: Comparison of numerical and experimental results of the axial viscoelastic response of UD CFRP at different temperatures; (a) Axial Young's modulus; (b) corresponding loss factor.

For the case of transverse loading (Fig. 7), the FE simulations effectively predict the observed dependence of the response on temperature and frequency. The experiments show a sensitivity to temperature slightly higher than that predicted by the FE simulations, however measurements and predictions are in good agreement.

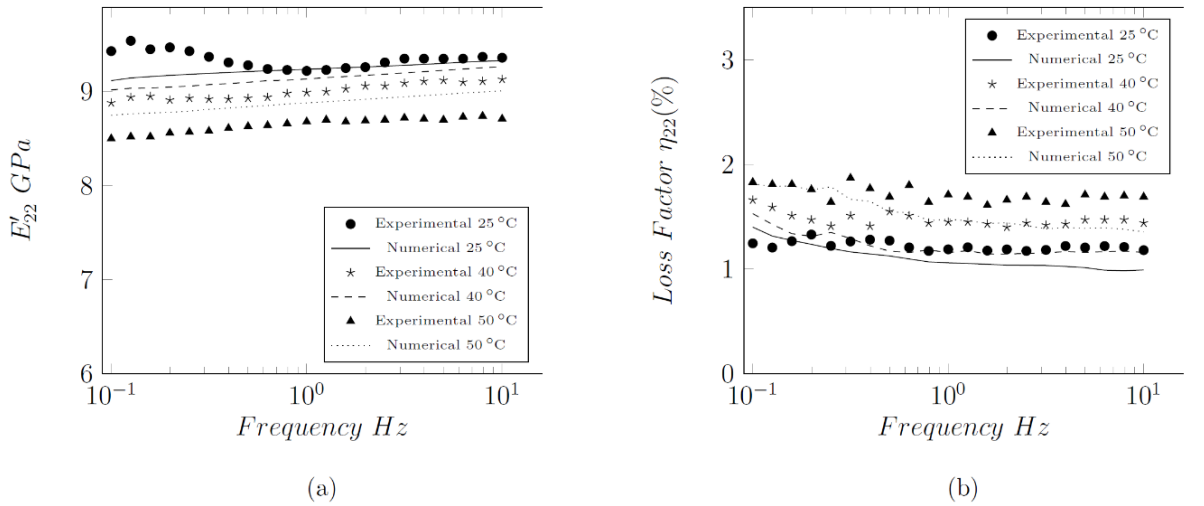

Figure 7: Comparison of numerical and experimental results of the transverse viscoelastic response of UD CFRP at different temperatures; (a) transverse Young's modulus; (b) corresponding loss factor.

In Fig. 8 we report measurements and predictions of the axial shear modulus and corresponding loss factor at different temperature and frequencies. Again the FE simulations capture correctly the effects of frequency and temperature observed in the experiments. A comparison of the numerical and experimental results is provided in Table 1 for the case of 1 Hz loading frequency and different temperatures.

4.3. New equations to predict the viscoelastic properties of a composite lamina

In the previous section we have validated the FE predictions conducted in this study against measurements on a composite of fibre volume fraction 0.63; we assume in the following that the FE predictions are able to capture the viscoelastic response of laminae of different volume fractions. We have also shown, in Section 4.1 and Figs. 3-5, that none of the theoretical models examined provides

accurate predictions for all viscoelastic properties. In this section we propose a new model to allow calculations of the viscoelastic properties with improved accuracy, using as input, the properties of the constituent materials.

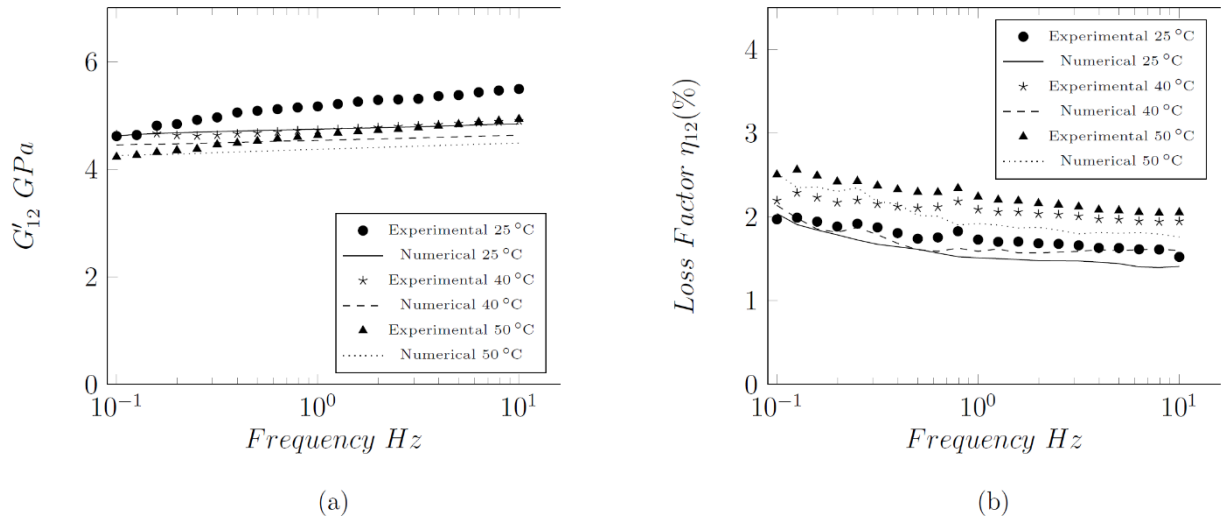

Figure 8: Comparison of numerical and experimental results of the axial shear viscoelastic response of UD CFRP at different temperatures; (a) Axial shear modulus; (b) corresponding loss factor.

	25°C		40°C		50°C	
	Numerical	Experimental	Numerical	Experimental	Numerical	Experimental
E_{11} (GPa)	140.75	138.64	141.21	136.64	140.84	133.00
E_{22} (GPa)	9.24	9.22	9.13	8.99	8.87	8.68
G_{12} (GPa)	4.74	5.17	4.53	4.72	4.37	4.63
η_{11} %	0.338	0.357	0.339	0.298	0.342	0.423
η_{22} %	1.05	1.18	1.15	1.45	1.47	1.71
η_{12} %	1.51	1.72	1.59	2.08	1.92	2.24

Table 1:Comparison of experimental results and numerical predictions of the anisotropic viscoelastic response of UD CFRP at 1 Hz frequency at 25, 40and 50° C.

The existing theoretical models which better captured the measured response were Mori-Tanaka and Lielens. We recall that while Mori-Tanaka is physically-based, the approach of Lielens [15] is to conduct a simple weighted averaging of the results of the Mori-Tanaka model [14] and of the Inverse Mori-Tanaka Tanaka model [6]. If the complex stiffness tensors predicted by the Mori-Tanaka (MT) and

Inverse Mori-Tanaka models are denoted by $C^*_{(MT)}$ and $C^*_{(IMT)}$, respectively, Lielens proposed a complex stiffness tensor calculated as

$$C^*_{LIELENS} = [(1 - f(\phi_f))C^{*-1}_{(MT)} + f(\phi_f)C^{*-1}_{(IMT)}]^{-1} \tag{2}$$

where $f(\phi_f)$ is a non-dimensional weighting function of the fibre volume fraction, ϕ_f. Based on the observation that experimental results tend to be closer to Mori-Tanaka model for low fibre volume fractions, while approach the Inverse Mori-Tanaka model at higher volume fractions, Lielens assumed $f(\phi_f) = (\phi_f + \phi_f{}^2)/2$; this choice however is not effective for the material investigated here. We therefore propose to use a different weighting function of general form

$$f(\phi_f) = \frac{1}{n}\sum_{i=1}^{n} \phi_f{}^i \tag{3}$$

We note that for $n = 2$ this equation coincides with that proposed by Lielens (eq. (3)). We proceed to find the optimal value of n which yields predictions in line with the validated FE calculations presented here, over a wide range of volume fractions. To do this, we perform additional simulations on RVEs of different volume fractions, in the range 0.2-0.7. For simplicity we consider a single temperature and frequency, arbitrarily chosen as 25 °C and 1 Hz, respectively. Ten repeated FE simulations were conducted for different loading cases, as shown in Figs 9-10. The figures include experimental measurements, for reference, and the theoretical predictions of the Lielens and Mori-Tanaka models. After a curve-fitting exercise on the data obtained, we find that the choice $n = 5$ provides a better fit through the results of FE predictions, for all loading cases. This corresponds to a complex stiffness tensor calculated as

$$C^*_{TP} = \left[(1 - \frac{1}{5}\sum_{i=1}^{5} \phi_f{}^i)C^{*-1}_{(MT)} + \left(\frac{1}{5}\sum_{i=1}^{5} \phi_f{}^i\right)C^{*-1}_{(IMT)}\right]^{-1} \tag{4}$$

The proposed C^*_{TP} tensor accurately predicts all viscoelastic lamina properties for the UD composite examined in this study.

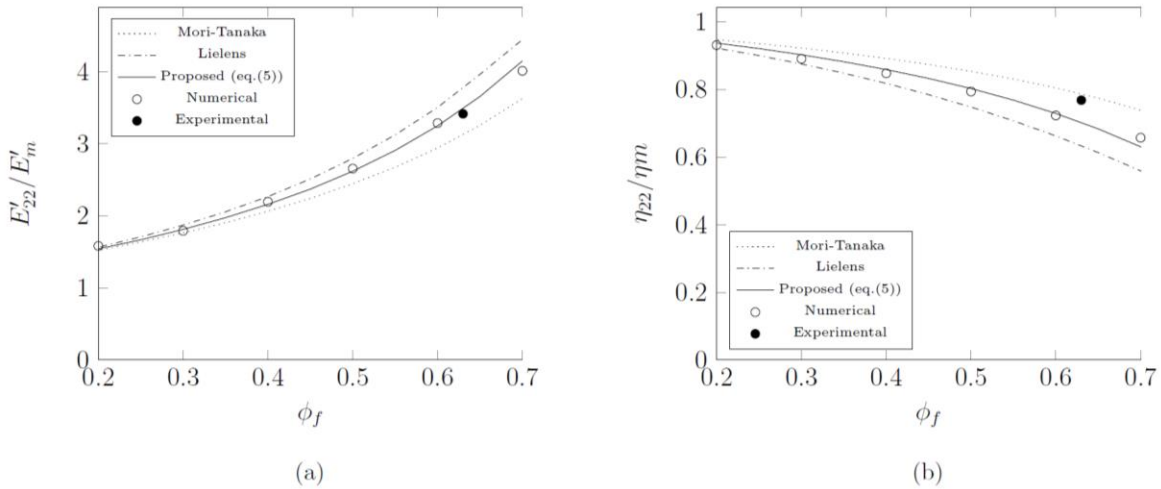

Figure 9: Comparison of the predictions obtained using the proposed analytical model to other methods for the case of transverse viscoelastic properties of UD CFRP as a function of fibre volume fraction; (a) Transverse Young's Modulus E'_{22}; (b) Corresponding loss factor η_{22}.

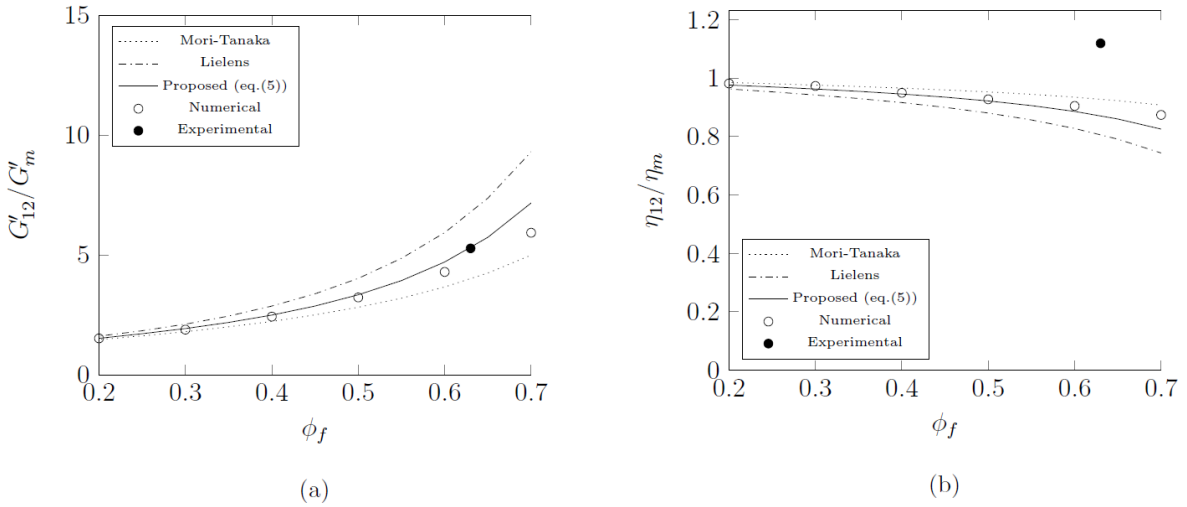

Figure 10: Comparison of the predictions obtained using the proposed analytical model to other methods for the case of axial shear viscoelastic properties of UD CFRP as a function of fibre volume fraction; (a) axial shear Modulus G'_{12}; (b) Corresponding loss factor η_{12}.

5. CONCLUSIONS

Measurements and FE predictions of the anisotropic viscoelastic response of a UD carbon composite were presented in this study. The validated FE predictions inspired the construction of new simple equations to provide accurate values of the viscoelastic properties of the UD composite. The concluding points of this study are follows:

- In all load cases, the macroscopic material stiffness increases with increasing imposed frequency and decreases with increasing temperature. Conversely, material damping decreases with increasing frequency and increases with increasing temperature. The axial modulus and corresponding loss factor are scarcely sensitive to frequency and temperature for the carbon fibre composite considered here.
- Conducting Monte Carlo analysis of repeated FE simulations of the response of random RVEs was shown to be an effective method to predict accurately the viscoelastic lamina properties at different frequency and temperature. Good agreement is found between numerical simulations and measurements in all loading cases; predictions of elastic properties are more accurate than those of loss factors, which are lower than measurements. The model was calibrated using exclusively the measured responses of the constituent materials and did not include any dissipation at the fibre-matrix interface; we deduce that this dissipation is not an important contributor to the loss factors of CFRP laminae, in the range of frequency and temperatures investigated.
- Several established theoretical models were tested against the experiments and the numerical predictions conducted in this study, and their accuracy was ranked. New equations were formulated to conduct accurate predictions of all the viscoelastic lamina properties of UD composites. These are expected to serve as a precious tool in prototyping, design and optimization of components made from fibre composites.

ACKNOWLEDGEMENTS

The authors would like to express gratitude to Sigmatex UK for providing the dry T700 carbon fibre fabric used in this study. This work is part of a collaborative R&T Project "SILOET II Project 10" which is co-funded by Innovate UK and Rolls-Royce plc and carried out by Rolls-Royce plc and Imperial College.

REFERENCES

[1] R. Rikards, A. Chate, A.K. Bledzki, V. Kushnevsky, Numerical modelling of damping properties of laminated composites, Mech. Compos. Mater. 30 (1994) 256–266.

[2] A.E. Mahi, M. Assarar, Y. Sefrani, J.-M. Berthelot, Damping analysis of orthotropic composite materials and laminates, Compos. Part B Eng. 39 (2008) 1069–1076. doi:10.1016/j.compositesb.2008.05.003.

[3] L.C. Brinson, W.S. Lin, Comparison of micromechanics methods for effective properties of multiphase viscoelastic composites, Compos. Struct. 41 (1998) 353–367.

[4] R. Chandra, S.P. Singh, K. Gupta, Micromechanical damping models for fiber-reinforced composites: a comparative study, Compos. Part Appl. Sci. Manuf. 33 (2002) 787–796.

[5] J.-L. Tsai, Y.-K. Chi, Effect of fiber array on damping behaviors of fiber composites, Compos. Part B Eng. 39 (2008) 1196–1204. doi:10.1016/j.compositesb.2008.03.003.

[6] M.V. Pathan, V.L. Tagarielli, S. Patsias, Numerical predictions of the anisotropic viscoelastic response of uni-directional fibre composites, Compos. Part Appl. Sci. Manuf. 93 (2017) 18–32. doi:10.1016/j.compositesa.2016.10.029.

[7] A.M. Figliolini, L.A. Carlsson, Mechanical properties of vinylester resins exposed to marine environments, Polym. Eng. Sci. 53 (2013) 2413–2421. doi:10.1002/pen.23496.

[8] C. Sauder, J. Lamon, R. Pailler, The tensile behavior of carbon fibers at high temperatures up to 2400 °C, Carbon. 42 (2004) 715–725. doi:10.1016/j.carbon.2003.11.020.

[9] S. Feih, A.P. Mouritz, Tensile properties of carbon fibres and carbon fibre–polymer composites in fire, Compos. Part Appl. Sci. Manuf. 43 (2012) 765–772. doi:10.1016/j.compositesa.2011.06.016.

[10] M.V. Pathan, V.L. Tagarielli, S. Patsias, P.M. Baiz-Villafranca, A new algorithm to generate representative volume elements of composites with cylindrical or spherical fillers, Compos. Part B Eng. (2016). doi:http://dx.doi.org/10.1016/j.compositesb.2016.10.078.

[11] A.R. Melro, P.P. Camanho, S.T. Pinho, Influence of geometrical parameters on the elastic response of unidirectional composite materials, Compos. Struct. 94 (2012) 3223–3231. doi:10.1016/j.compstruct.2012.05.004.

[12] Z. Hashin, On elastic behaviour of fibre reinforced materials of arbitrary transverse phase geometry, J. Mech. Phys. Solids. 13 (1965) 119–134.

[13] R. Hill, Theory of mechanical properties of fibre-strengthened materials: I. Elastic behaviour, J. Mech. Phys. Solids. 12 (1964) 199–212.

[14] T. Mori, H. Tanaka, Average stress in matrix and average elastic energy of materials with misfitting inclusions, Acta Metall. 21 (1973) 571–574.

[15] G. Lielens, P. Pirotte, Prediction of thermo-mechanical properties for compression moulded composites, Compos. Part Appl. Sci. Manuf. 29 (1998) 63–70.